Magnetotelluric response and geoelectric structure of the Great Slave Lake shear zone

Xianghong Wu [a,*], Ian J. Ferguson [a], Alan G. Jones [b]

[a] *Department of Geological Sciences, University of Manitoba, Winnipeg, MB, R3T 2N2, Canada*
[b] *Geological Survey of Canada, 615 Booth St, Ottawa, ON, K1A 0E9, Canada*

Abstract

The Great Slave Lake shear zone (GSLsz) is a northeast-trending 25-km-wide dextral continental transform fault from the foothills of the Rocky Mountains in northeast British Columbia to the southeast side of Great Slave Lake. Based on its magnetic expression the GSLsz can be correlated for at least 1300 km, mostly in the subsurface. Magnetotelluric (MT) soundings were made at 60 sites in the southwest part of the Northwest Territories, Canada, along the LITHOPROBE Slave–Northern Cordillera Lithospheric Evolution (SNORCLE) Transect Corridors 1 and 1A, in the Summer and Autumn of 1996. Of these, 15 sites were along Corridor 1A which crossed the GSLsz, the Great Bear magmatic arc and Hay River terrane to the northwest of the shear zone, and the Buffalo Head terrane to the southeast. The primary objective of the Corridor 1A deployments was to image the structure of the GSLsz. Analysis of MT data indicates that along the Corridor 1A the resistivity structure is approximately 1D at shallow depth (<1 km) corresponding to Phanerozoic sedimentary rocks, 2D in the upper to mid crust with a strike $\sim$N30°E, and approximately 2D in the lower crust to lithospheric mantle with a strike of $\sim$N60°E. The direction in the upper crust is interpreted to represent the local-scale (<50 km) horizontal strike of the GSLsz whereas the direction in the mantle is parallel to the larger-scale strike of the GSLsz. 2D inversions of the MT data reveal that the GSLsz forms a crustal-scale resistive zone (>5000 Ωm) that is spatially correlated with a magnetic low. The GSLsz comprises greenschist to granulite facies mylonites. Its high resistivity is interpreted to be due to the resistive nature of the granitic protolith of the mylonites and that mylonites are dominated by rocks deformed in the ductile regime. To the northwest of GSLsz the MT profile reveals crustal conductors beneath the Great Bear magmatic arc and Hay River terrane. The enhanced conductivity occurring beneath the Great Bear magmatic arc is interpreted to be caused by electronic conduction within deformed and metamorphosed rocks of the Hottah terrane or the Coronation Supergroup. The MT results also reveal a mantle conductor beneath the margin of the Hottah terrane and Great Bear magmatic arc that is interpreted to be associated with the subduction of oceanic lithosphere. A second mantle conductor to the southeast is truncated at the GSLsz suggesting an older source for the enhanced conductivity and that the GSLsz includes significant strike–slip motion of sub-crustal lithosphere. © 2002 Elsevier Science B.V. All rights reserved.

Keywords: Great Slave Lake; shear zones; Paleoproterozoic; Rae Province; lithosphere

* Corresponding author. Fax: +1-204-474-7623.
E-mail addresses: umwux@cc.umanitoba.ca (X. Wu), ij_ferguson@umanitoba.ca (I.J. Ferguson), ajones@nrcan.gc.ca (A.G. Jones).

1. Introduction

The LITHOPROBE Slave–Northern Cordillera Lithospheric Evolution (SNORCLE) Transect Corridor 1A, located south of Great Slave Lake, Northwest Territories, Canada (Fig. 1), crosses Proterozoic terranes interpreted to lie beneath the thin veneer of Paleozoic sediments. These terranes are the Great Bear magmatic arc, the Hay River terrane and the Buffalo Head terrane, and the interpretation is based primarily on aeromagnetic data, chips from basement-reaching boreholes, and extrapolations of surface outcrop to the north [1]. The Paleoproterozoic Great Slave Lake shear zone (GSLsz), arguably the most dominant linear feature on the aeromagnetic map of Canada, is located between the Hay River and Buffalo Head terranes and was proposed by Hanmer [2] as the type example of a crustal-scale continental shear zone.

One specific objective of the SNORCLE transect investigations was to determine the geometry and lithospheric extent of the GSLsz, given its continental scale, so an appropriately designed magnetotelluric (MT) survey was undertaken. The MT method has been used successfully to investigate major fault systems, and examples include the Fraser [3] and the Slocan Lake faults [4] in southern British Columbia, the Tintina-northern Rocky Mountain Trench fault in northern British Columbia and the Yukon [5], the Denali fault of the Yukon and Alaska [6], the San Andreas fault in California [7–9], and the Alpine fault on the southern island of New Zealand [10,11].

In MT investigations depth information is obtained using the period variation of the response: signals of different period penetrate to different depths into the earth. Short-period MT signals (10^{-4}–10^{-3} s) penetrate several hundred meters into the earth whereas long-period signals (10^3–10^4 s) penetrate 100 km or more into the upper mantle. The period range in the present study extends from 10^{-4} to 10^4 s allowing imaging of the surface Paleozoic sedimentary rocks, the Precambrian crust, and the lithospheric mantle.

In this paper we will present analyses and interpretation of the MT data acquired across the GSLsz. We will examine the variation of the geoelectric strike direction with depth, variation of the resistivity across the GSLsz, and lithospheric structure. We will demonstrate that the shear zone is characterized by a resistive zone at crustal depths, that the shear zone extends through the crust, and that there is an associated electrical conductivity signature in the underlying mantle lithosphere. In a companion study to this one Eaton et al. [12] examined the teleseismic response on a profile crossing the GSLsz. Their preliminary results are discussed below.

2. Geological setting

The GSLsz is a northeast-trending 25-km-wide dextral continental transform fault, with up to 700 km of strike–slip motion, extending from the foothills of the Rocky Mountains in northeast British Columbia to the southeast side of Great Slave Lake [13]. It is linked to the convergence and collision between the Archean Slave and Rae provinces in the Paleoproterozoic and developed in arc environment associated with the initial subduction of Slave lithosphere [13–15]. Based on its magnetic expression the GSLsz can be correlated for at least 1300 km, mostly in the subsurface. Ductile displacement on the GSLsz is estimated to have been up to 700 km. U–Pb zircon ages on syntectonic granites define a minimum duration for ductile shear of 2.03 to 1.95 Ga [13]. Where it is exposed along the southeast shore of Great Slave Lake, the GSLsz comprises granulite to lower greenschist facies mylonite belts [13,15]. In areas where it is exposed the GSLsz zone has a width of about 25 km [2,15].

Post-collisional convergence of the Slave and Rae provinces at ca. 1.8 Ga [16] produced an additional 75–125 km of strike–slip motion on the McDonald fault system (MF). The overall trend of the MF is coincident with the GSLsz, but at a smaller-scale the MF consists of a series of an echelon brittle displacements connected by transpressional transfer zones that cut the GSLsz [15]. Along Corridor 1A the GSLsz and MF are covered by Devonian sedimentary rocks. The corridor crosses a distinct magnetic low that has a
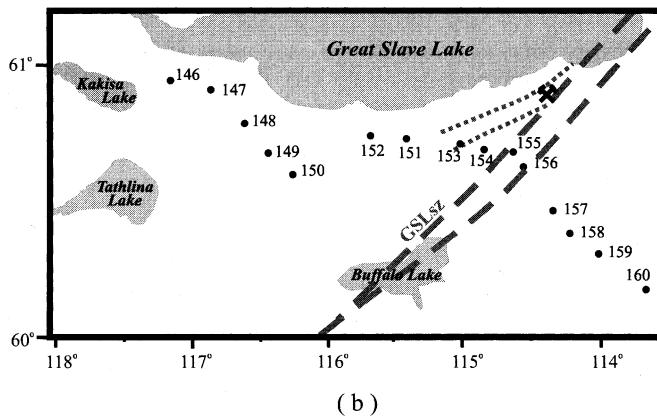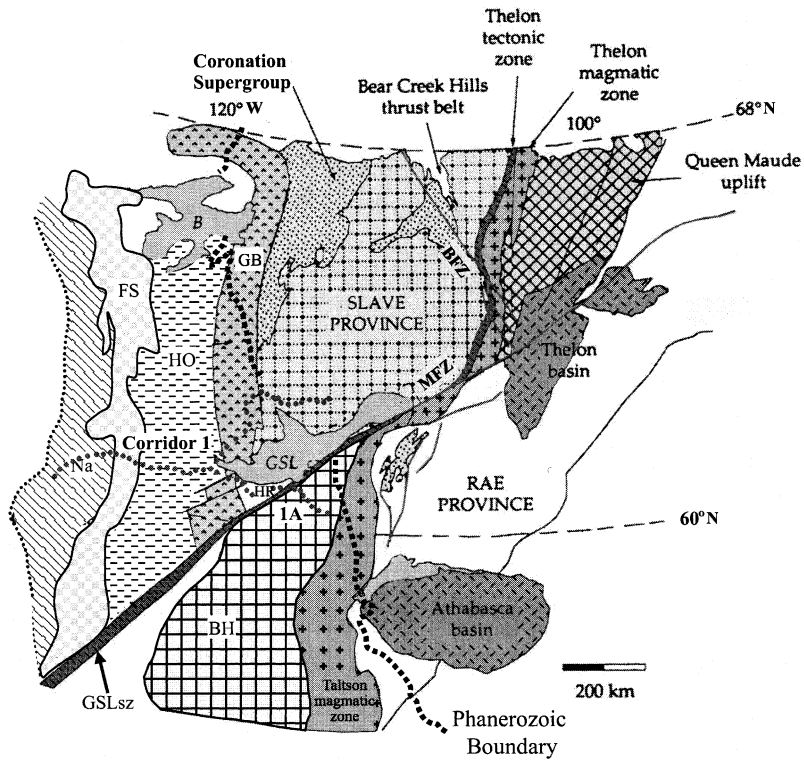
(a)

(b)

Fig. 1. (a) Selected tectonic elements and structures of the northwest Canadian Shield (after Hanmer, 1988). Na: Nahanni terrane, FS: Fort Simpson terrane, HO: Hottah terrane, GB: Great Bear magmatic arc, HR: Hay River terrane, GSLsz: Great Slave Lake shear zone, BH: Buffalo Head terrane, BFZ: Bathurst fault zone, MFZ: McDonald fault zone. The circles show the location of MT sites on Corridor 1 and 1A. (b) Location of sites along Corridor 1A. The location of the GSLsz is shown by dashed lines and is inferred from magnetic field data. The dotted line shows the location of the Pine Point (Presqu'ile) barrier. The mine symbol shows the location of the Pine Point Mine.

width of about 30 km, and, on the basis of its similarity to the magnetic response of the exposed GSLsz, this magnetic low is interpreted to be the location of the GSLsz.

At the location of the LITHOPROBE profile, the geological terranes to the northwest of the fault are the Great Bear magmatic arc and the Hay River terrane and the terrane to the southeast of the fault is the Buffalo Head terrane (Fig. 1). The Proterozoic Great Bear magmatic arc is a continental 'calc–alkalic' volcano–plutonic depression dated at 1.875–1.84 Ga that uncomfortably overlies the Hottah terrane and/or (deformed) Coronation margin strata [17,18]. The geological structure of the Hay River terrane is poorly known as the terrane is not exposed at the surface. Drill-core and potential field results indicate that the terrane consists of granitic material and corresponds to a magnetic low [19]. The Buffalo Head terrane is a 2.4–2.0 Ga magmatic belt [1]. It comprises metaplutonic and subordinate felsic metavolcanic rocks [1]. The north-trending Taltson magmatic zone (1.99–1.90 Ga) welds the Buffalo Head terrane to the east [20] and is a belt of granitic to dioritic plutons (1.99–1.92 Ga).

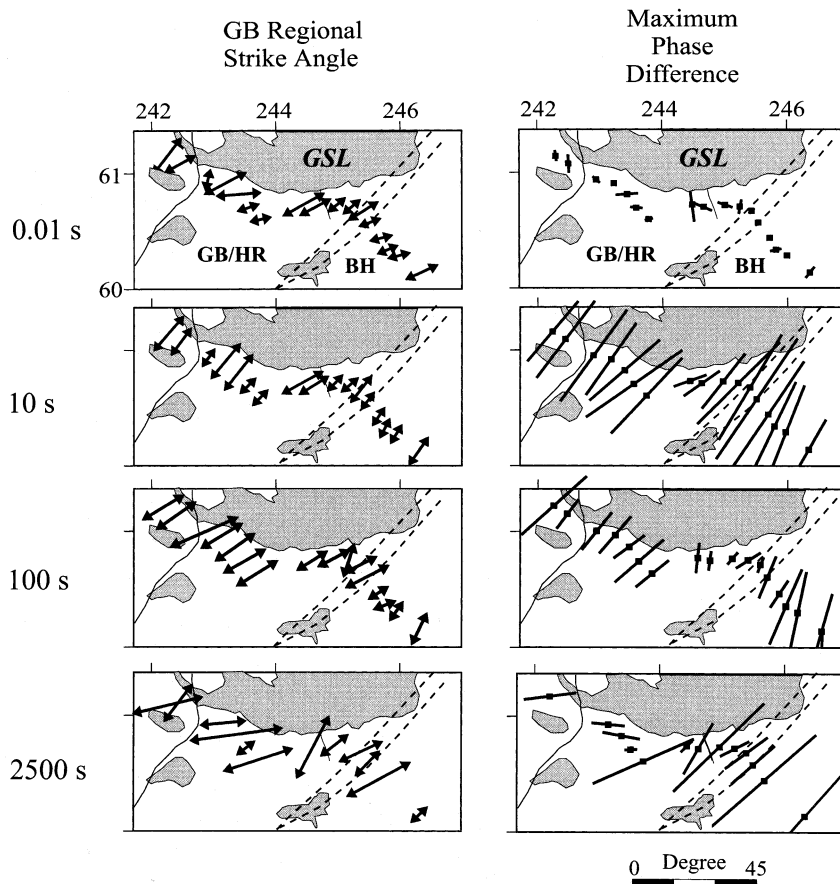Along Corridor 1A the Precambrian rocks are overlain by 300–700 m of Devonian sedimentary

Fig. 2. The Groom–Bailey regional strike and maximum phase split orientations along the SNORCLE Transect Corridor 1A at 0.01 s, 10 s, 100 s and 2500 s. There is a 90° ambiguity between the direction of the orientations and the true strike. The resolution scale on the GB plot, represented by the length of the strike symbol, is inversely proportional to misfit χ^2 error between the GB decomposition impedances and the observed impedances. The strike angle plot excludes several sites for which the strike angle was unresolved.

rocks. These rocks dip gently to the west at 1.9 m per km [21]. To the northwest of the GSLsz Corridor 1A obliquely crosses a 10-km-wide Middle to Upper Devonian barrier complex, the Pine Point barrier, which forms part of the larger-scale Presqu'ile Barrier separating the Devonian Elk Point Basin in the south from the Mackenzie Basin in the north. The Pine Point barrier hosts the major Mississippi Valley type Pb-Zn Pine Point deposit that is located approximately 25 km north of the corridor [21]. The overburden in the survey area consists of ∼20 m of Holocene and Pleistocene sediments (e.g. [21]).

3. MT survey and data analysis

Soundings at 60 MT sites were completed along SNORCLE transect Corridor 1 and Corridor 1A in the southwest Northwest Territories, Canada in the Summer and Autumn of 1996 [22]. There are 15 sites on Corridor 1A (Fig. 1). Sites 155 and 156 lie above the interpreted location of the GSLsz but the magnetic low extends over much of the distance between 154 and 157 (Fig. 2). Sites 154 and 153 lie on a sigmoidal-shaped magnetic high forming the eastern margin of the magnetic low. Sites 153 to 152 lie above or adjacent to the Pine Point barrier.

The MT recordings included Phoenix V5 measurements (10^{-4}–100 s) at all sites and Geological Survey of Canada long-period MT responses (LiMS) measurements (20–30 000 s) at all sites except 158 and 159. The MT recordings included measurement of time-variations of the horizontal electric and magnetic fields in orthogonal directions and of the vertical magnetic field. Recordings from adjacent or nearby sites were used as the remote reference for noise reduction.

The Jones–Jödicke approach [23,24] and the Chave approach [25] were used for time series processing to yield the MT response functions. Particular attention was placed to correct the LiMS data for distortion due to non-uniform source fields associated with auroral geomagnetic activity [26]. The V5 and LiMS data were merged in order to obtain an 8-decade-period range (10^{-4}–10^{4} s). The MT responses determined from the recorded time series include the MT impedance, apparent resistivity and phase. The MT impedance is a tensor quantity relating the two horizontal components of the electric field to the horizontal components of the magnetic field in the frequency domain. Each tensor term can be used to estimate an apparent resistivity, a spatially averaged resistivity over the penetration depth of the signals. The phase of the impedance, the phase lead of the electric over the magnetic field, also provides information on the underlying resistivity structure.

4. Geoelectric strike directions

The MT impedance tensor can be used to determine the dimensionality and strike of the resistivity structure. In the maximum phase split method, whereby the impedances are rotated to determine the greatest phase difference between the off-diagonal elements, the geoelectric strike is determined as the orientation in which the phase difference between off-diagonal impedance tensor elements is maximized. Electric charge accumulation on near-surface heterogeneities can distort the measured MT response so that it no longer accurately represents the larger-scale (regional) conductivity structure. In the Groom–Bailey (GB) tensor decomposition method [27,28] the geoelectric strike is determined simultaneously with the near-surface distortion effects using a least-squares approach.

The geoelectric strikes in the study area were derived using GB tensor decomposition and the maximum phase-split method at periods of 0.01 s, 10 s, 100 s and 2500 s (Fig. 2,3). The maximum phase split results are for a narrow band of periods centered on these values, whereas the GB results are for a one-decade-wide band. The penetration depth of the signals at these periods can be estimated using electromagnetic skin depth relations or the method of Schmucker and Janknowsky [29] which estimates the depth of the "centre of mass" of the subsurface electric current distribution.

The MT signals at period 0.01 s correspond to penetration depths of ∼300 m in the southeast of

the profile and $\sim$ 50 m in the northwest. At this period, the maximum phase differences are small ($< 10°$) at all sites (Fig. 2) implying little lateral heterogeneity in the shallow subsurface beneath each site. The GB regional strike direction is weakly defined with an average direction of $\sim$ N60°E along the profile (Fig. 3). At most sites the ratio of the apparent resistivity corresponding to the MT response in the two orthogonal directions is between 0.85 and 1.20 [22] indicating the departures from a 1D or layered MT response are small. Because of inherent ambiguity the geoelectric strike may be perpendicular or parallel to the azimuth determined from GB analysis and the true strike may be $\sim$ N30°W. This direction corresponds well with the strike of the Phanerozoic sedimentary rocks (Fig. 2) so it is probable that the weak 2D response is associated with the gentle westward dip of the sedimentary rocks.

A 10-s period corresponds to an upper crustal signal penetration of 5 km to the northwest of the GSLsz and about 17 km for sites to the southeast of the GSLsz. At this period the GB regional

strike has an orientation of N32°E at most sites but an orientation closer to N45°E at sites 151 and 152 near the middle of the profile (Figs. 2 and 3). The maximum phase orientation is well resolved and is similar to the GB regional strike. A 100-s period corresponds to penetration of MT signals to around 30 km depth in the northwest, and > 55 km to the southeast, of the GSLsz. The GB regional strike direction is approximately N56°E at sites crossing the GSLsz but rotates to N29°E at the southeast end of the profile (Figs. 2 and 3). The maximum phase difference direction is $\sim$ N45°E at sites in the Great Bear magmatic arc, but again rotates to about N20°E at sites in the Buffalo Head terrane near the southeast end of the profile.

MT signals at periods of > 1000 s penetrate through the deepest crust and into the sub-continental lithospheric mantle. Because of the lower signal to noise ratio at these periods, the GB strike and maximum phase difference directions are more erratic (Fig. 2). The GB regional strike direction has an average orientation of N65°E

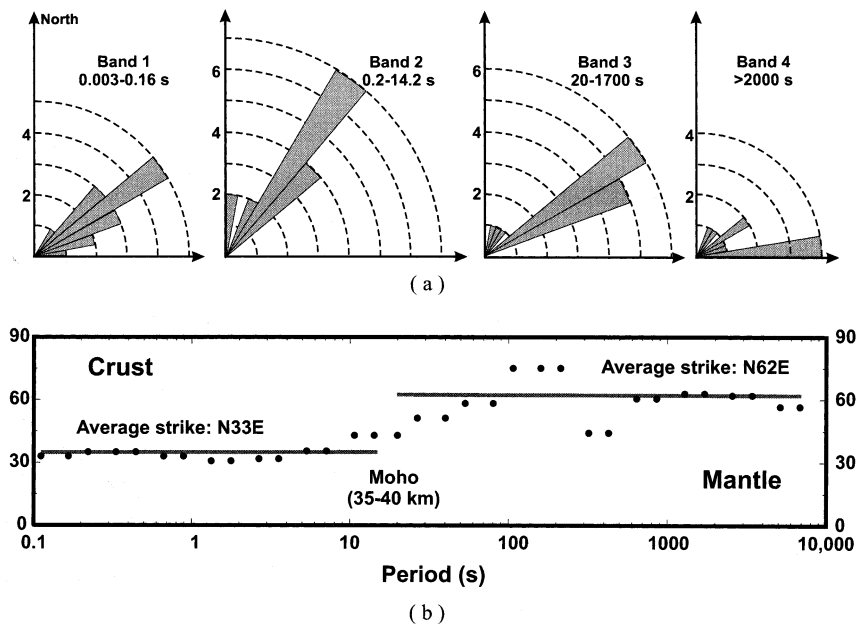Fig. 3. (a) Rose diagram of the GB regional strike angle for four period ranges based on the 15 sites along Corridor 1A. The angle bin is 10°. The results for the first two period bands include 15 resolved strikes angles, the results for band 3 include 14 strikes, and for band 4 include 10 strikes. (b) Geoelectric strike angle from multisite, multifrequency extended GB decomposition that best fits all sites along Corridor 1A simultaneously.

across the profile but has a more east–west orientation within the Great Bear magmatic arc. The average maximum phase direction at southeast sites on the profile is N140°E but because of an inherent 90° ambiguity this direction is likely perpendicular to the geoelectric strike.

At periods longer than 1 s the GB regional strike and maximum phase split results are moderately consistent (to within ±15°) at different sites and at different periods and indicate an approximately 2D structure along the profile. However, the results do resolve a change in strike angle with period from a strike of ∼N32°E at 10 s to ∼N65°E at >1000 s indicating a 3D component in the data. The strike angle variation can be further investigated using the McNeice–Jones [30] multisite, multifrequency extended GB decomposition to determine the geoelectric strike angle that best fits all sites along Corridor 1A simultaneously. The results of this analysis are shown in Fig. 3. Short periods (0.1–10 s) show a preference for a strike scattering in the range N30°–35°E, whereas long periods (>60 s) scatter in the range N45°–75°E. Multisite, multifrequency analysis in two period bands results in a short-period strike of N33°E and a long-period strike of N62°E. The transition between these two directions initiates in the period range 10–20 s, which is approximately the period range for sensitivity of the MT signals to the lower crust.

5. MT apparent resistivity and phase responses

The GB tensor decomposition results provide a measure of the distortion of the MT response: the GB shear provides a measure of the local polarization of the electric field. At sites along Corridor 1A the shear angle is <5° at periods <1 s, indicating an absence of near-surface inhomogeneities. At periods >30 s the shear at most sites is in the range 10°–30° indicating moderate distortion. The GB distortion parameters vary consistently from site to site indicating the source of the distortion is the large-scale structure rather than local heterogeneities. Near-surface effects can cause a static shift of the MT responses that cannot be resolved in the GB analysis. The static shift

was analyzed using methods proposed by Jones [31] and Sternberg et al. [32] that established the static shift using multiple sites along the profile [22]. The resulting static shift correction factors are small at all sites, typically in the range 0.75–1.3. Accordingly, we exclude static shift corrections in the following processing.

The MT response in a 2D structure can be divided into two independent modes involving electric current flow parallel to strike, the transverse electric or TE mode, and electric flow perpendicular to strike, the transverse magnetic or TM mode [33]. In the present study the TE component is defined to have an orientation of N41°E, the average strike angle over the period range 0.02–200 s. This represents an average of the short-period (N33°E) and long-period (N62°E) strike directions shown in Fig. 3. Models obtained in those strike directions showed essentially the same features discussed below. Fig. 4 shows the apparent resistivity and phase responses for the TE and TM mode.

At periods of <0.1 s corresponding to signal penetration to several hundred meters both the TE and TM response show a decrease in resistivity with increasing period (and thus depth). The phase exceeds 45° as expected for cases in which the resistivity decreases with depth. At periods of 0.1–1000 s corresponding to signal penetration into the Precambrian crust the TE and TM apparent resistivities are significantly higher than at shorter period. The TE and TM responses are quite similar and both indicate that the apparent resistivity in the Buffalo Head terrane (>400 Ωm) is higher than that in the Great Bear magmatic arc (<400 Ωm). The TE and TM responses differ from each other near sites 155 and 156 indicating stronger 2D features. In the period range 0.3–3 s the part of the profile between sites 153 and 156 is characterized by relatively high TE phase (with a local low at site 155) and by relatively low TM phase. The apparent resistivity exhibits corresponding effects over the period range 3–100 s with the TE response being relatively conductive (locally more resistive at 155) and the TM response being relatively resistive. The responses suggest the presence of resistive crust beneath site 155.
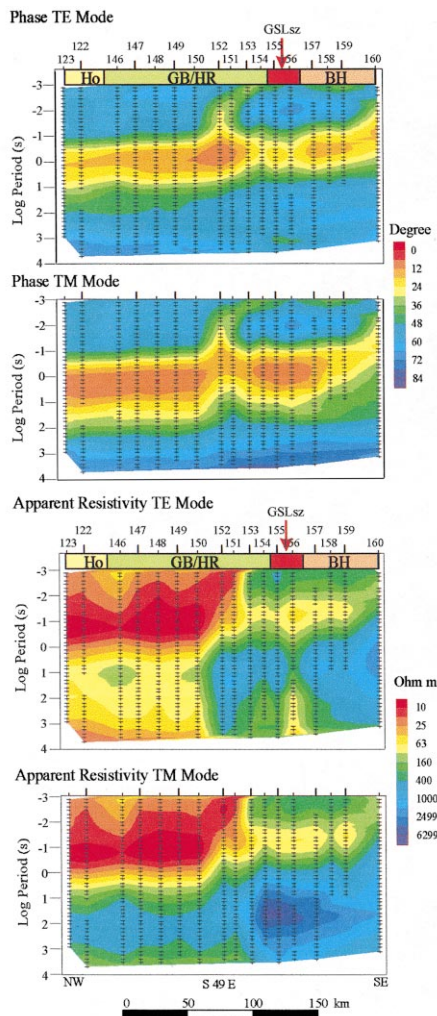
Fig. 4. Apparent resistivity and phase pseudosections for the TE and TM modes along Corridor 1A. The profile is perpendicular to regional geoelectrical strike N41°E. Crosses show the location of data points. The data have been corrected for distortion using a GB model.

At very long periods (> 1000 s) there is a decrease in the apparent resistivity beneath the Hottah terrane and the Great Bear magmatic arc and a corresponding increase in the phase. These responses indicate the presence of a conductive layer at mantle depth beneath these geological units. The same MT responses are not visible in the Buffalo Head terrane indicating an absence of, or greater depth from, this conductor.

6. Resistivity structure

The 2D OCCAM [34] and non-linear conjugate gradient (NLCG) [35] inversion methods were used to determine the resistivity structure of the Precambrian lithosphere. As discussed above, the geoelectric strike direction varies with period and therefore depth around the GSLsz. In order to examine the strike dependence of MT models
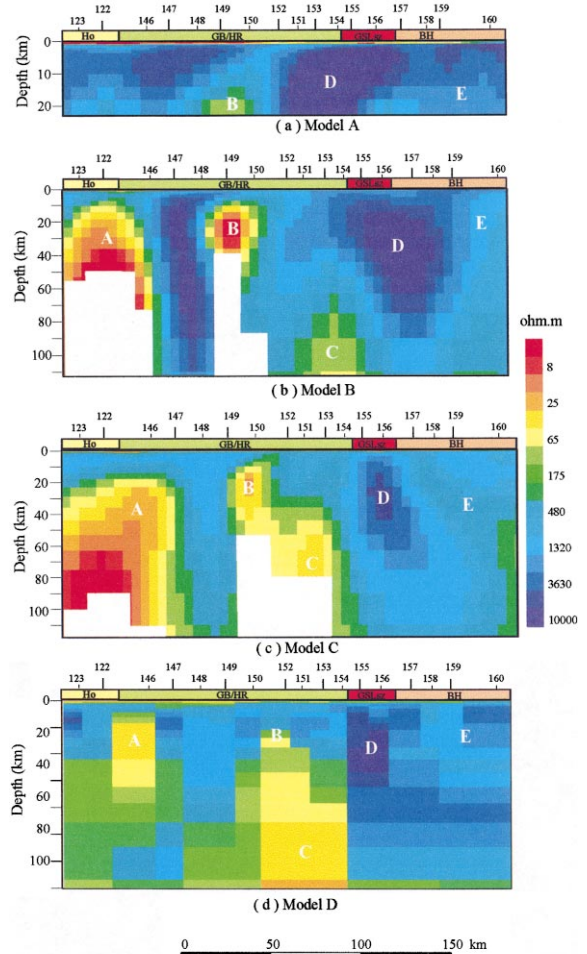

Fig. 5. Four inversion models along Corridor 1A.(a) NLCG inversion for data at periods < 10 s at 30° strike angle, (b) NLCG inversion for data at periods > 30 s at 60° strike angle, (c) NLCG inversion for data at periods 0.001–3000 s at 41° strike angle. (d) Occam inversion for data at periods 0.001–3000 s with 41° strike angle. There is no signal penetration in the blanked area.

from the upper crust to the upper mantle across the GSLsz, inversions of MT data from the different period ranges and with the different strike angle were completed (Table 1). An inversion model obtained using short-period data (< 10 s) and a N30°E rotation angle is designed to resolve upper to middle crustal structure (Model A). The resolution depth for a period of 10 s is less than 20 km. An inversion model obtained using long-period data (30–3000 s) and N60°E rotation angle is designed to resolve middle to lower crust and upper mantle structure (Model B). Very similar results are obtained when the starting model for this inversion includes near-surface resistivity structures (< 1 km) defined by the higher frequency (N30°E) inversion, when it includes upper crustal resistivity structures (< 20 km) defined by the higher frequency inversion, and when the upper crustal structure is fixed to the results of the higher frequency inversion. Finally, inversions obtained using a full period range (10^{-3}–3000 s) and average rotation angle N41°E are designed to resolve the structure from the near-surface to mantle (Models C and D) and to stitch the results from the other two inversions.

Multiple inversions were done using different inversion parameters and different subsets of the data. Fig. 5 shows the four final inversion models obtained using both TE and TM data. The responses of Model C are shown for representative sites in Fig. 6. The model provides a reasonably good fit to the data: the root mean square misfit, based on error floors of 5% for the apparent resistivity data and 1.4° (equivalent to 2.5% in apparent resistivity) for the phase data, is 4.5. This means that we are fitting the data to $\sim 6°$ in phase, on average. The TE data show the poorest fits, at periods longer than 10 s at sites 150, 151, 154, 155, and particularly 156. Investigation of

the site 156 response shows that for a range of TE directions, between N30°E and N60°E, the GB distortion parameters at periods exceeding 10 s are relative high and frequency-dependent. Also, in a series of 2D inversions, e.g. using decreased error floors relative to other sites, it was not possible to obtain a good combined fit to both TE and TM responses at site 156. These results suggest the presence of a more complex crustal structure near the center of the profile. Modelling studies have shown that the TM response is more robust than the TE response in the presence of local 3D structures [36,37] so the superior fit to the TM response provides increased confidence in the models.

The structures in the final models are robust features that appear in most of the inversions. The major geoelectric structures in the model are labelled A–D and are discussed below.

- There is a conductive zone (~ 30 Ωm) in the lower crust beneath the boundary of the Hottah terrane and Great Bear magmatic arc (labelled A). Seismic reflection results indicate the depth to the Moho on Corridor 1 at its intersection with Corridor 1A is ~ 40 km [17]. The MT images suggest that the conductive zone extends into the mantle but the depth of its base within the mantle is not well resolved. There is a sharp eastern edge to the conductive zone at site 147.
- There is a conductive zone (labelled B) with its top at ~ 15 km depth below sites 149 and 150. The conductivity of the body is < 50 Ωm in models B, C and D and its thickness is at least 20 km. Its presence is supported by the observations in the apparent resistivity pseudosections (Fig. 4) which show moderately low resistivity at periods of 10–1000 s beneath sites 149 and 150. The conductor is located near the interpreted position of the Hay River terrane and Great Bear magmatic arc (Fig. 1).
- There is a conductive zone (labelled C) at mantle depths beneath sites 150–154. The resistivity of the zone reaches values of < 100 Ωm in all of the models. The upper surface of the zone appears to have an eastward dip. In some models this conductor connects with the previous

Table 1
2D Inversions for Corridor 1A data using different strike angles

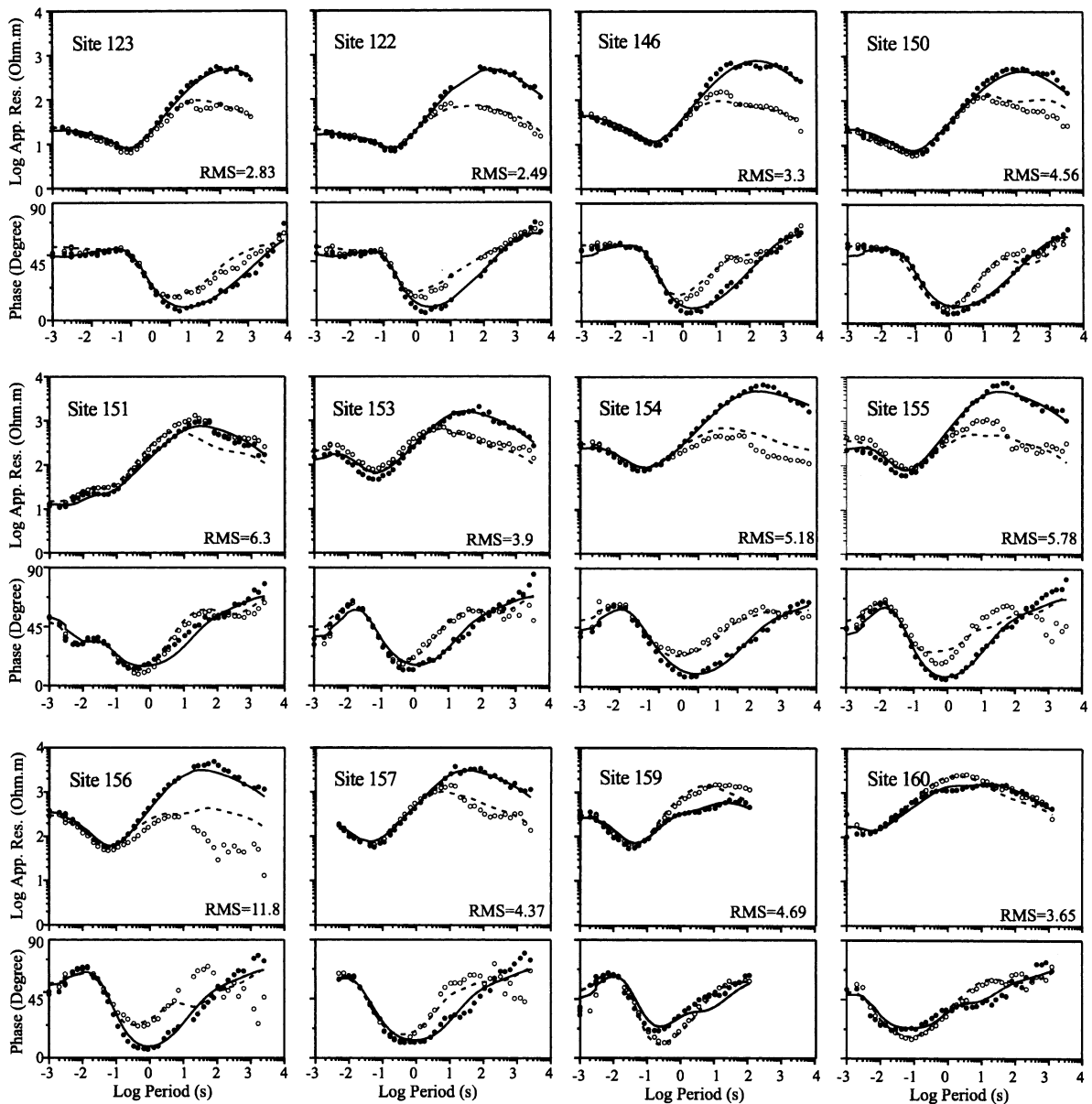| Model	Inversion period	Rotation angle	Inversion method
A	10^{-3}–10	N30°E	NLCG
B	30–3000	N60°E	NLCG
C	10^{-3}–3000	N41°E	NLCG
D	10^{-3}–3000	N41°E	OCCAM

Fig. 6. Comparison of the NLCG inversion model apparent resistivity and phase responses with the observed data at some representative sites. Solid line: TM response, dash line: TE response, ●: TM observed data, ○: TE mode observed data. The RMS misfit for each site for Model C (Fig. 5) is shown.

conductor but this aspect is not well resolved. The southeastern margin of this conductor at sites 154 and 155 consists of a sharp transition to more resistive zone to the southeast.

● There is a sub-vertical resistive zone ($\sim$10 000 Ωm) beneath sites 155 and 156, labelled D. For

all inversions of data sets extending to periods of at least 100 s, and for data rotations of N30°E, N41°E, and N60°E, the resulting models include a resistive zone extending through the crust. The exact configuration of the resistive zone depends on the rotation of the data

inverted. For models derived from data with a N30°E rotation angle (model A) the resistor extends further to the northwest than for models derived from data with a N60°E rotation (model B). It is of note that none of the models fits the more conductive TE response at site 156, but as noted above, the models do provide a good fit to the TM mode data at this site and the misfit to the TE mode is interpreted to be due to local 3D structures. Overall, the results permit the conclusion that the MT data require the presence of a resistive zone centered on sites 155 and 156.

7. Geological interpretation

7.1. Great Bear magmatic arc–Hay River terrane

The Great Bear magmatic arc has been interpreted by Cook et al. [18] as the product of eastward subduction of oceanic lithosphere beneath the Hottah terrane at 1.84–1.87 Ga. Cook et al [18] suggest that the Great Bear magmatic arc is relatively thin ($\sim$3–4.5 km) and lies above either Hottah crust or imbricated rocks of the Coronation margin. Therefore, the enhanced conductivity in the middle and the lower crust beneath the boundary between the Hottah terrane and Great Bear magmatic arc (labelled A in Fig. 5) corresponds to deformed and metamorphosed rocks of either the Hottah terrane or the Coronation Supergroup. The source of the enhanced conductivity could be either carbon or conductive minerals concentrated during the deformation and metamorphism. In studies of rocks from the Kapuskasing uplift [38] and Trans-Hudson orogen [39], petrophysical models and MT results have suggested graphite can be a source to enhance the conductivity of mid-lower crust. Alternatively, Gupta and Jones [40] and Jones et al. [41] discuss extensive conductivity anomalies in the crust caused by interconnected sulphide mineralization. In either case, the enhanced conductivity is caused by electronic conduction in interconnected metasediments. The source of the high crustal conductivity observed to the southeast is less certain, particularly because of uncertainty in the bound-

ary between the Great Bear magmatic arc and the Hay River terrane.

7.2. GSLsz

2D MT modelling results reveal a sub-vertical resistive zone ($> 3000\ \Omega$m) in the upper-lower crust beneath sites 155 and 156, which is coincident with the magnetic anomaly low (Fig. 5, 7). The resistive zone is interpreted to represent the electrical signature of the GSLsz.

Interpretation of the resistive response of the GSLsz requires consideration of the geology of the shear zone. Where the GSLsz is exposed to the northwest it has been mapped as a bundle of upright belts of mylonites [15]. The mylonites are interpreted to have been formed from a mixed protolith of hornblende-biotite, magnetite-bearing, granite and granodiorite that was intruded both pre- and syntectonically. The oldest mylonites are of granulite facies and formed a belt with a width of > 10 km, possibly up to 25 km. The metamorphic grade of the mylonites decreases with decreasing age with the decreasing grade reflecting both decreases in temperature and pressure [2]. The subsequent strain produced progressively narrowing belts of upper and lower amphibolite grade mylonite and lower greenschist-facies chlorite-bearing mylonites. The late
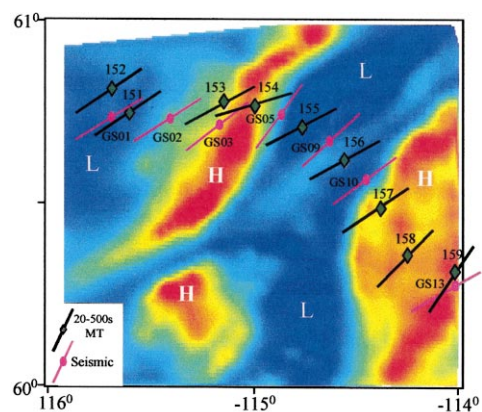

Fig. 7. Comparison of magnetic field data, long-period MT azimuths, and SKS fast directions. The H and L symbols refer to magnetic highs and lows respectively. The MT strikes are for the period band 20–500 s.

stage of deformation evolved through the ductile–brittle transition and the latest stages involved dilational faulting and development of quartz stockworks [2,15].

The relatively high resistivity of the GSLsz suggests that at the location of the LITHOPROBE Corridor all of the mylonite units have high electrical resistivity. Within the GSLsz on the exposed shield greenschist facies mylonite occurs in a network of belts up to 2 km wide and 70 km long. If such greenschist facies mylonites occur within the study area they must have relatively high resistivity. This result is consistent with a detailed study by Olhoeft [42] who found that structural water provided little contribution to the electrical conductivity. It is also possible that the effective electrical conductivity of the lower grade mylonite belts is also reduced by the presence of a quartz 'stockwork' which consists of vertical veins up to 25 m wide and up to 40 km long that cut the mylonite structures [2].

Studies of major transcurrent faults have provided evidence for both conductive and resistive fault zones. The Tintina fault in the northern Cordillera is a major fault with up to 450 km of dextral transcurrent movement [5]. MT results show that the fault is associated with a 20 km wide resistive zone (>400 Ωm) at depths exceeding 5 km. The Denali fault in Alaska is also associated with relatively resistive rocks at upper crustal depths [6] and the San Andreas fault at Carrizo Plain is associated with a resistive zone at midcrustal depths [7]. In contrast the MT results from elsewhere on the San Andreas fault [8] and from other major transcurrent faults including the Alpine fault in New Zealand [10] and the Fraser fault in British Columbia, Canada [3] have a conductive signature.

A variety of sources of the enhanced conductivity within fault and shear zones have been proposed. These include clays and other minerals associated with the faulting process [8], graphite precipitated from fluids within the fault [3], and in the case of active faults, fluids present in the fault zone. Serpentinite has also been proposed in the case of faults involving oceanic rocks and a degree of dip slip movement [8]. The results from the GSLsz imply the absence of any of these components over a region of $\sim$20 km width extending throughout the crust.

The high resistivity of the GSLsz can be attributed to the composition of the protolith, the conditions of the deformation and to subsequent fluid movements and reactions. The protolith for the mylonitized rocks, at least to the northwest of the study area, is horneblende-biotite granite [2]. In its undeformed state this rock would be relatively resistive [21]. The rocks within the GSLsz are dominated volumetrically by mylonites formed at granulite to amphibolite metamorphic grade within a ductile rheology. Deformation occurring under these metamorphic conditions would be less likely to create enhanced conductivity than brittle faulting at lower metamorphic grade that could be associated with the formation of clay minerals with high cation exchange capacities and enhanced conductivity. The granulite facies metamorphism may have released fluids through dehydration reactions but such fluids could have either been consumed in retrograde reactions [43] or may have dissipated over the long time period since the deformation.

7.3. Sub-crustal lithosphere

The MT responses and 2D inversion models all show a region of enhanced conductivity at depth. The maximum depth to the 150 Ωm contour in the 2D Occam models is $\sim$150 km and occurs in the Buffalo Head terrane. This depth is interpreted to correspond to the base of the lithosphere with the enhanced conductivity at greater depth explained by a small component of more conductive partial melt in the asthenosphere. The enhanced conductivity observed at shallow mantle depths beneath the boundary of the Hottah terrane and Great Bear magmatic arc (labelled A in Fig. 5) and to the northwest of the GSLsz (labelled B in Fig. 5) is more localized and is therefore interpreted to represent increased conductivity within the lithosphere rather than a decrease in lithospheric thickness.

Seismic reflection results show delamination structures extending to 100 km depth in the mantle beneath the Great Bear magmatic arc providing evidence that lower crustal rocks were em-

placed in the mantle during subduction [17,18] associated with collision and accretion of the Hottah terrane to the western margin of the Slave craton between 1.94 and 186 Ga. Bostock and Cassidy [44] also suggest on the basis of teleseismic and heatflow data that the lithospheric mantle beneath the east and southeast of the Slave province has been reworked through processes associated with subduction and continental collision. The source of the enhanced conductivity in the mantle beneath the western Great Bear magmatic arc may be either hydrogen or carbon introduced into the mantle through the subduction process.

There is a significant boundary in the mantle conductivity at the GSLsz with the conductivity being higher to the northwest of the boundary. The precise geometry of this boundary is rather poorly constrained by the MT data because it is occurring at the longest periods available in the response and is obscured in part by the overlying crustal structures. Nevertheless the existence of the conductive mantle to the northwest of the GSLsz is supported by the observed high phases and low apparent resistivity at periods exceeding 10^3 s at sites northwest of 154 (Fig. 4). The truncation of the mantle conductor near the GSLsz suggests significant strike–slip movement of mantle lithosphere as well as the crust. However, the movement on the GSLsz (2.03–1.95 Ga) predates the recorded orogenic activity associated with the collision of the Hottah terrane and Slave province (1.94–1.86 Ga) [13]. If the high mantle conductivity truncated by the shear zone was caused by the subduction of oceanic lithosphere it suggests that, either some subduction occurred before 1.94 Ga or else, there was relative motion at lithospheric depth on the shear zone subsequent to 1.95 Ga. The most probable explanation is that the truncation of the conductor is explained by the movement on the younger (ca. 1.8 Ga) MF.

8. Discussion

The MT responses define clear azimuthal dependence in the area of the GSLsz. The geoelectric strike changes from ∼N33°E at periods corresponding to the upper crust to N62°E at periods corresponding to lithospheric penetration. The geoelectric strike in the crust is more north–south than the regional (>40 km scale) strike of the GSLsz south of Slave province which is N60°E [15]. However, the magnetic low also suggests an azimuth similar to the MT results (Fig. 7). The results suggest that the strike of the GSLsz where it crosses Corridor 1A is locally close to N30°E. Deflections of the shear zone away from the regional N60°E azimuth are observed on the exposed portion of the GSLsz to the northwest. Hanmer [2] attributes such deflections to late stage deformation wrapping around constrictions.

There is the possibility that the magnetic anomaly on Corridor 1A represents a transpressional transfer zone of the MF rather than the GSLsz. The transfer zones strike between N30°E to N50°E, consistent with the strike of the magnetic anomaly. However, the 30 km width of the anomaly, and its similarity with the magnetic anomaly of GSLsz on the exposed shield, together support the interpretation of the GSLsz as the source rather than the MF. The presence of an electrically resistive structure strengthens this interpretation, as it is more difficult to explain the observed high resistivity if it is associated with brittle faulting.

The geoelectric strike at periods corresponding to signal penetration to lithospheric depths is N62°E. This orientation is parallel to both the larger-scale strike of the GSLsz to the south of the Slave province and to the larger-scale strike of the MF. The result suggests the tectonic motion associated with these faults has been recorded by the resistivity structure of the mantle lithosphere.

In a companion study to the present one, Eaton et al. [12] resolve significant shear wave splitting near the GSLsz with differences in SKS arrival times from different azimuths of 1.1–1.5 s. There is consistency between the fast axis at each site with an average direction of approximately N50°E (Fig. 7). This direction is sub-parallel to the absolute plate motion direction of 225° suggesting that the observed seismic anisotropy may be due to present-day asthenospheric flow. The small obliquity between the directions is possibly

due to localized deflections caused by topography at the base of the lithosphere [12].

These shear wave splitting data are interpretable in terms of two-layer seismic anisotropy [12] and the different geoelectric strike directions determined at short and long periods (Fig. 3) provide support for such a two-layer interpretation. Preliminary two-layer inversions of the seismic data (D. Eaton, personal communication, 2001) suggest an upper layer with a polarization subparallel to the short-period MT strike at short periods and a lower layer with a polarization oblique to both the long period MT strike and to absolute plate motion.

At sites near the Grenville Front in eastern Canada, an average 23° obliquity between SKS and MT responses has been interpreted by Ji et al. [45] as a kinematic indicator of dextral shearing. The seismic and MT anisotropies are thought to be caused by lattice-preferred and shape-preferred orientation of mantle minerals respectively [45]. In the area of the GSLsz there is an obliquity between the average MT strike direction of N62°E, at periods corresponding to mantle penetration, and the seismically determined SKS fast axis for a single layer of N50°E. This obliquity is particularly evident within the magnetic low interpreted to represent the GSLsz and within the magnetic high to the northwest (Fig. 7). This obliquity we would interpret to be a consequence of the seismic anisotropy being due to present-day asthenospheric flow and the MT strike being associated with Paleoproterozoic lithospheric structures.

However, if two-layer seismic analysis leads to the seismic anisotropy being interpreted in terms of a lithospheric source, then comparison of the MT and seismic data will provide an important assessment of the model of Ji et al. [45].

9. Conclusions

Analyses of the MT data collected on a profile crossing the GSLsz along the SNORCLE Transect Corridor 1A have shown that the geoelectric strike direction near the GSLsz varies with depth from ∼N33°E at periods less than 20 s corre-
sponding to the upper and middle crust to ∼N62°E at period range of 20–1500 s corresponding to the lower crust and lithospheric mantle. These results and 2D modelling show that the GSLsz is a lithospheric-scale feature. Within the crust the GSLsz forms a resistive zone at least 20 km wide and at the surface is correlated with a magnetic low. The rocks within the GSLsz consist of greenschist to granulite facies mylonites. The high resistivity ($>5000 \; \Omega m$) is interpreted to be due to the resistive nature of the granitic protolith of the mylonites and the fact that the GSLsz are dominated volumetrically by rocks deformed within the ductile regime.

The geoelectric strike at crustal depths in the vicinity of the GSLsz is more north–south than the overall azimuth of the shear zone to the south of the Slave province (N60°E) but is consistent with the strike of the magnetic anomaly interpreted to correspond to the shear zone. This strike is interpreted to reflect a local-scale (<50 km) deflection of the mylonite belts. The geoelectric strike at periods corresponding to lower crust and mantle lithosphere depths is N62°E. This orientation is close to the large-scale (>50 km) azimuth of the shear zone south of the Slave province. In the present study the long-period MT responses were fitted quite well by a resistivity model consisting of 2D isotropic structures but the data could also be fitted by a model incorporating both anisotropic conductors and structural elements.

from S. Constable and C. deGroot-Hedlin as implemented in the Geotools software package. The magnetic data were provided by the GSC. Paul Hoffman, Malcolm Ingham, Juanjo Ledo, and an anonymous reviewer are thanked for their constructive comments. LITHOPROBE contribution 1261, GSC contribution 2001158.*[RV]*

References

[1] G.M. Ross, R.R. Parrish, M.E. Villeneuve, S.A. Bowring, Geophysical and geochronology of the crystalline basement of the Alberta Basin, western Canada, Can. J. Earth Sci. 28 (1991) 512–522.

[2] S. Hanmer, Great Slave Lake shear zone, Canadian Shield: reconstructed vertical profile of a crustal-scale fault zone, Tectonophysics 149 (1988) 245–264.

[3] A.G. Jones, R.D. Kurtz, D.E. Boerner, J.A. Craven, G.W. McNeice, D.I. Gough, J.M. DeLaurier, R.G. Ellis, Electromagnetic constraints on strike-slip geometry – The Fraser River fault system, Geology 20 (1992) 561–564.

[4] A.G. Jones, D.I. Gough, Electromagnetic images of crustal structures in southern and central Canadian Cordillera, Can. J. Earth Sci. 32 (1995) 1541–1563.

[5] J. Ledo, A.G. Jones, I.J. Ferguson, Electromagnetic images of a strike-slip fault: the Tintina Fault-northern Canadian Cordillera, Geophys. Res. Lett. (2002) in press.

[6] W.D. Stanley, V.F. Labson, W.J. Nokleberg, B. Csejtey, M.A. Fisher, The Denali fault system and Alaska Range of Alaska: evidence for underplated Mesozoic flysch from magnetotelluric surveys, Geol. Soc. Am. Bull. 102 (1990) 160–173.

[7] R.L. Mackie, D.W. Livelybrooks, T.R. Madden, J.C. Larsen, A magnetotelluric investigation of the San Andreas Fault at Carrizo Plain, California, Geophys. Res. Lett. 24 (1997) 1847–1850.

[8] M.J. Unsworth, P.E. Malin, G.D. Egbert, J.R. Booker, Internal structure of the San Andreas Fault at Parkfield California, Geology 25 (1997) 359–362.

[9] M.J. Unsworth, G.D. Egbert, J.R. Booker, High-resolution electromagnetic imaging of the San Andreas Fault in Central California, J. Geophys. Res. 104 (1999) 1131–1150.

[10] M. Ingham, C. Brown, A magnetotelluric study of the Alpine Fault, New Zealand, Geophys. J. Int. 135 (1998) 542–552.

[11] F.J. Davey, T. Henyey, W.S. Holbrook, D. Okaya, T.A. Stern, A. Melhuish, S. Henrys, H. Anderson, D. Eberhart-Phillips, T. McEvilly, R. Uhrhammer, F. Wu, G.R. Jiracek, P.E. Wannamaker, G. Caldwell, N. Christensen, Preliminary results from a geophysical study across a modern, continent-continent collisional plate boundary; the Southern Alps, New Zealand, Tectonophysics 288 (1998) 221–235.

[12] D. Eaton, I. Asudeh, I.A. Jones, Mantle strain beneath the Great Slave Lake Shear Zone, NWT from measurements of seismic and electrical anisotropy, in: F. Cook, P. Erdmer (Eds.), Slave-Northern Cordillera Lithospheric Evolution (SNORCLE) Transect and Cordilleran Tectonics Workshop Meeting, February, University of Calgary, AB, LITHOPROBE Report, 72, 2000, 56–63

[13] P.F. Hoffman, Continental transform tectonics Great Slave Lake shear zone (1.9 Ga), northwest Canada, Geology 15 (1987) 785–788.

[14] R.A. Gibb, Slave–Churchill collision tectonics, Nature 271 (1978) 50–52.

[15] S. Hanmer, S. Bowring, O. Breemen, R. Parrish, Great Slave Lake shear zone, NW Canada: mylonitic record of early Proterozoic continental convergence, collision and indentation, J. Struct. Geol. 14 (1992) 757–773.

[16] B.D. Ritts, J.P. Grotzinger, Depositional facies and detrital composition of the Paleoproterozoic Et-Then Group, NWT, Canada: sedimentary response to intracratonic indentation, Can. J. Earth Sci. 31 (1994) 1763–1778.

[17] F.A. Cook, A.J. VanderVelden, K.W. Hall, B.J. Roberts, Tectonic delamination and subcrustal imbrication of the Precambrian lithosphere in northwestern Canada mapped by LITHOPROBE, Geology 26 (1998) 839–842.

[18] F.A. Cook, A.J. VanderVelden, K.W. Hall, B.J. Roberts, Frozen subduction in Canada's Northwest Territories Lithoprobe deep lithospheric reflection profiling of the western Canadian Shield, Tectonics 18 (1999) 1–24.

[19] G.M. Ross, H.C. Annell, M.A. Hamilton, Lithology and U–Pb geochronology of shallow basement along the SNORCLE line, southwest Northwest Territories: A preliminary report, in: F. Cook, P. Erdmer, (Eds.), Slave-Northern Cordillera Lithospheric Evolution (SNORCLE) Transect and Cordilleran Tectonics Workshop Meeting, February, University of Calgary, AB, LITHOPROBE Report, 72, 2000, 76–80.

[20] R.J. Thériault, Nd isotopic evidence for Paleoproterozoic pre-Taltson magmatic zone (1.99–1.90 Ga) rifting of western Churchill Province, in: G.M Ross (Ed.) Lithoprobe Alberta basement transects workshop meeting, February, Ramada Hotel, Calgary, AB, LITHOPROBE Report, 37, 1994, 267–269.

[21] D. Rhodes, E.A. Lantos, J.A. Lantos, R.J. Webb, D.C. Owens, Pine Point orebodies and their relationship to the stratigraphy, structure, dolomitization, and karstification of the Middle Devonian Barrier Complex, Econ. Geol. 79 (1984) 991–1055.

[22] X. Wu, Determination of near-surface, crustal, and lithospheric structure in the Canadian Precambrian Shield using the time-domain electromagnetic and magnetotelluric methods, Ph.D. Thesis, University of Manitoba, Winnipeg, MB, 2001.

[23] A.G. Jones, H. Jödicke, Magnetotelluric transfer function estimation improvement by a coherence-based rejection technique, Contributed paper at 54th Ann. Int. Meeting, Soc. Explor. Geophys., Atlanta, GA, Dec. 2–6, 1984, Expanded abstracts 51–55.

[24] A.G. Jones, A.D. Chave, G. Egbert, D. Auld, K.K. Bahr, A comparison of techniques for Magnetotelluric response function estimation, J. Geophys. Res. 94 (1989) 14201–14213.

[25] A.D. Chave, D.J. Thomson, Some comments on magnetotelluric response function estimation, J. Geophys. Res. 94 (1989) 14215–14225.

[26] X. Garcia, A.D. Chave, A.G. Jones, Robust processing of magnetotelluric data from the auroral zone, J. Geomagn. Geoelectr. 49 (1997) 1451–1468.

[27] G.W. Groom, R.C. Bailey, Decomposition of magnetotelluric impedance tensors in the presence of local three-dimensional galvanic distortion, J. Geophys. Res. 94 (1989) 1913–1925.

[28] R.W. Groom, R.D. Kurtz, A.G. Jones, D.E. Boerner, A quantitative methodology to extract regional magnetotelluric impedances and determine the dimension of the conductivity structure, Geophys. J. Int. 115 (1993) 1095–1118.

[29] U. Schmucker, J. Janknowsky, Geomagnetic induction studies and the electrical state of the upper mantle, Tectonophysics 13 (1972) 233–256.

[30] G. McNeice, A.G. Jones, Multisite, multifrequency tensor decomposition of magnetotelluric data, Geophysics 66 (2001) 158–173.

[31] A.G. Jones, Static shift of magnetotelluric data and its removal in a sedimentary basin environment, Geophysics 53 (1988) 967–978.

[32] B.K. Sternberg, J.C. Washburne, L. Pellerin, Correction for the static shift in magnetotellurics using transient electromagnetic soundings, Geophysics 53 (1988) 1459–1468.

[33] K. Vozoff, The magnetotelluric methods, in: M.N. Nabighian (Ed.), Electromagnetic Methods in Applied Geophysics, vol. 2 Applications, Society of Exploration Geophysicists, Tulsa, OK, 1991, 641–711.

[34] C. deGroot-Hedlin, S. Constable, Occam's inversion to generate smooth, two-dimensional models from magnetotelluric data, Geophysics 55 (1990) 1613–1624.

[35] W. Rodi, R.L. Mackie, Nonlinear conjugate gradients algorithm for 2-D magnetotelluric inversion, Geophysics 66 (2001) 174–187.

[36] A.G. Jones, The problem of 'current channeling': a critical review, Geophys. Surv. 6 (1983) 79–122.

[37] P.E. Wannamaker, G.W. Hohmann, S.H. Ward, Magnetotelluric responses of three-dimensional bodies in layered earths, Geophysics 49 (1984) 1517–1533.

[38] T.J. Katsube, M. Mareschal, Petrophysical model of deep electrical conductors: graphite lining as a source and its disconnection due to uplift, J. Geophys. Res. 98 (1993) 8019–8030.

[39] A.G. Jones, J.A. Craven, The north American central plains conductivity anomaly and its correlation with gravity, magnetic, seismic, and heat flow data in Saskatchewan, Canada, Phys. Earth Planet. Inter. 60 (1990) 169–194.

[40] J.C. Gupta, A.G. Jones, Electrical conductivity structure of the Purcell Anticlinorium in southeast British Columbia and northwest Montana, Can. J. Earth Sci. 32 (1995) 1564–1583.

[41] A.G. Jones, J. Katsube, P. Schwann, The longest conductivity anomaly in the world explained: sulphides in fold hinges causing very high electrical anisotropy, J. Geomagn. Geoelectr. 49 (1997) 1619–1629.

[42] G.R. Olhoeft, Electrical properties of granite with implications for the lower crust, J. Geophys. Res. 86 (1981) 931–936.

[43] B.W.D. Yardley, Is there water in the deep continental crust?, Nature 323 (1986) 111.

[44] M.G. Bostock, J.F. Cassidy, Upper mantle stratigraphy beneath the southern Slave craton, Can. J. Earth Sci. 34 (1997) 577–587.

[45] S. Ji, S. Rondenay, M. Mareschal, G. Senechal, Obliquity between seismic and electrical anisotropies as a potential indicator of movement sense for ductile shear zones in the upper mantle, Geology 24 (1996) 1033–1036.